Geomaterials, 2016, 6, 61-77
Published Online July 2016 in SciRes. http://www.scirp.org/journal/gm
http://dx.doi.org/10.4236/gm.2016.63006

Scientific Research Publishing

Geochemical Characterization of the Paleocene Ewekoro Limestone Formation, SW Nigeria: Implications for Provenance, Diagenesis and Depositional Environment

O. Ajayi Ehinola[1], O. Innocent Ejeh[2], O. Justine Oderinde[1]

[1]Department of Geology, University of Ibadan, Ibadan, Nigeria
[2]Department of Geology, Delta State University, Abraka, Nigeria
Email: ehinola01@yahoo.com

Received 31 March 2016; accepted 17 July 2016; published 20 July 2016

Abstract

The usefulness of limestone as an industrial raw material is dependent on the level of its purity, largely controlled by diagenesis and the depositional setting. Limestone samples (83) obtained from the Ewekoro Formation exposed in quarry sections at Shagamu were analyzed using X-Ray Fluorescence spectrometry (XRF). A geochemical characterization of result was done to evaluate the purity levels and the implications on provenance, diagenesis, and depositional setting of the limestone. Five limestone beds from quarry sections (15 locations) were logged. Beds "E", "D", "C", "B", and "A" comprised sandy algal in sparry calcite cement, sandy biomicrite, algal biomicrite, sandy algal biomicrite, and the intra-sparite facies respectively. Results of major elements chemistry indicated concentrations (in wt%) as follows: CaO (33.71 - 59.99), MgO (0.39 - 3.15), Al_2O_3 (0.47 - 3.23), Fe_2O_3 (0.51 - 3.43), SiO_2 (0.47 - 45.98), SO_3 (0.10 - 2.27), K_2O (0.02 - 0.28), Na_2O (0.00 - 10.0), TiO_2 (0.00 - 0.27), P_2O_5 (0.02 - 0.92), MnO (0.01 - 0.06) and Loss on ignition (17.64 - 45.20). Geochemical result showed that the samples are enriched in CaO, while SiO_2 varies widely, likely due to hinterland input. Plots of SiO_2 versus CaO concentrations depicted a negative correlation attributable to chemical diagenetic processes. Diagenesis of the carbonate in form of reversible replacement of SiO_2 with CaO and vice versa occurred under a shallow marine condition. This negative correlation between these oxides (CaO and SiO_2) dictates zones of high purity limestones that are of desirable industrial applications. Relatively high silica content in the northwestern part is possible indication of outlets to the continental or inland areas where clastic sediment source may have been prominent. Ratios of Ca/Mg and Mg/Ca indicated a relatively low rate of evaporation of sea water and palaeo-salinity conditions marked by precipitation of limestone. Intermittent increase in palaeo-salinity and sea water evaporation level gave rise to the magnesian limestone.

How to cite this paper: Ehinola, O.A., Ejeh, O.I. and Oderinde, O.J. (2016) Geochemical Characterization of the Paleocene Ewekoro Limestone Formation, SW Nigeria: Implications for Provenance, Diagenesis and Depositional Environment. *Geomaterials*, **6**, 61-77. http://dx.doi.org/10.4236/gm.2016.63006

Keywords

Geochemical Characterization, Ewekoro Formation, Ca/Mg Ratio, Limestone, Carbonate, Silica

1. Introduction

Carbonate rocks constitute about 50% of the world's hydrocarbon reservoir rocks, and among these limestones are widely used as raw materials in the chemical, metallurgical and construction industries. The quality and hence the usefulness of limestone deposit is largely dependent on the geological setting and the physico-chemical, mechanical and mineralogical characteristics of the stone. An evaluation of usefulness or appraisal of a limestone deposit entails a geological field investigation and laboratory analyses of representative samples. Naturally, limestone carries varied suite of impurities such as SiO_2, MgO and Fe_2O_3, whose geochemical concentration determines its industrial application(s). Therefore an assessment of its grade through geochemical analyses such as XRF is essential. Most limestone industrial applications consider the carbonate and MgO contents as fundamental criteria for its chemical purity or grade classification.

In accord with the global increase in the applications of geological models for exploration and exploitation of mineral resources; geochemical models revealing limestone's chemical purity can be used as a tool to appraise the spatio-temporal distribution of limestone purity throughout the deposit. The modelling approach is targeted at locating anomalous concentration(s) of high purity limestone or other pathfinder elements and characterizing the host lithologies. This method may form a basis for comparison of data for limestones of other geological settings all over the earth.

The Ewekoro limestone belt extends to the northwest and beyond Shagamu to the southeastern part of the embayment. Nwajide [1] reported the limestone reserve estimate of [2] of about 36 million tons. Reyment [3] also presented estimated values of chemical constituents of quarried limestones from the Ewekoro as follows: CaO (53%), CO_2 (42%), SiO_2 (2%), Al_2O_3 (5%), Fe_2O_3 (1.4%), P_2O_5 (0.8%), MgO (0.3%), MnO (0.1%), and minor quantities of Na_2O, K_2O, TiO_2, F and trace of SO_3. Although, these geochemical reports are some five decades old and some of the relatively recent related studies include those of [4]-[7] and others; but not much has been done on geochemical characterization to re-appraise the spatio-temporal variation of elemental compositions of the carbonates. This study examines the geochemical characteristics of the Paleocene Ewekoro limestone Formation; using results from XRF analysis of samples obtained in order to determine provenance, diagenesis and depositional setting of the study area. The study area lies within Latitudes 6˚47'N to 6˚48'N and Longitudes 3˚38'E to 3˚39'E, the present location of the Shagamu quarry (**Figure 1**).

2. Geological Setting

2.1. Tectonic Framework

The Dahomey Embayment spans the continental margin of the Gulf of Guinea, covering the Volta delta in Ghana to the west and the Okitipupa ridge/Benin hinge line to the east [8] [9]. It's a marginal pull-apart basin or marginal sag basin [10] that developed in the Mesozoic sequel to the separation of African from the South American plates [11] [12]. This separation, accompanied by basement fracturing accounted for the early rifting stage during Jurassic to Early Cretaceous and the development of several marginal sub-basins [9].

2.2. Stratigraphy

The eastern Dahomey Embayment (**Figure 1**) has been studied both on outcrop scale as well as from core holes by various workers such as [2] [4] [8] [9] [13]-[16], amongst others. The stratigraphy of the Nigerian sector of the embayment can be broadly divided into two: the Cretaceous Abeokuta Group (comprising Ise, Afowo and Araromi Formations) and the Cenozoic units (comprising Ewekoro, Akinbo, Oshoshun, Ilaro, and Benin Formations) [2] [9] (**Figure 2**). However, this study is focused on the Ewekoro limestone Formation.

This formation is made up of fossiliferous shelly limestone of about 12.5 meters thick, which tends to be sandy at the base [1]. It has been divided into three micro-facies namely: the sandy biomicrite lower unit; the shelly biomicrite grading into biomicrosparite middle unit that consists mainly of pure limestone making up the bulk of the

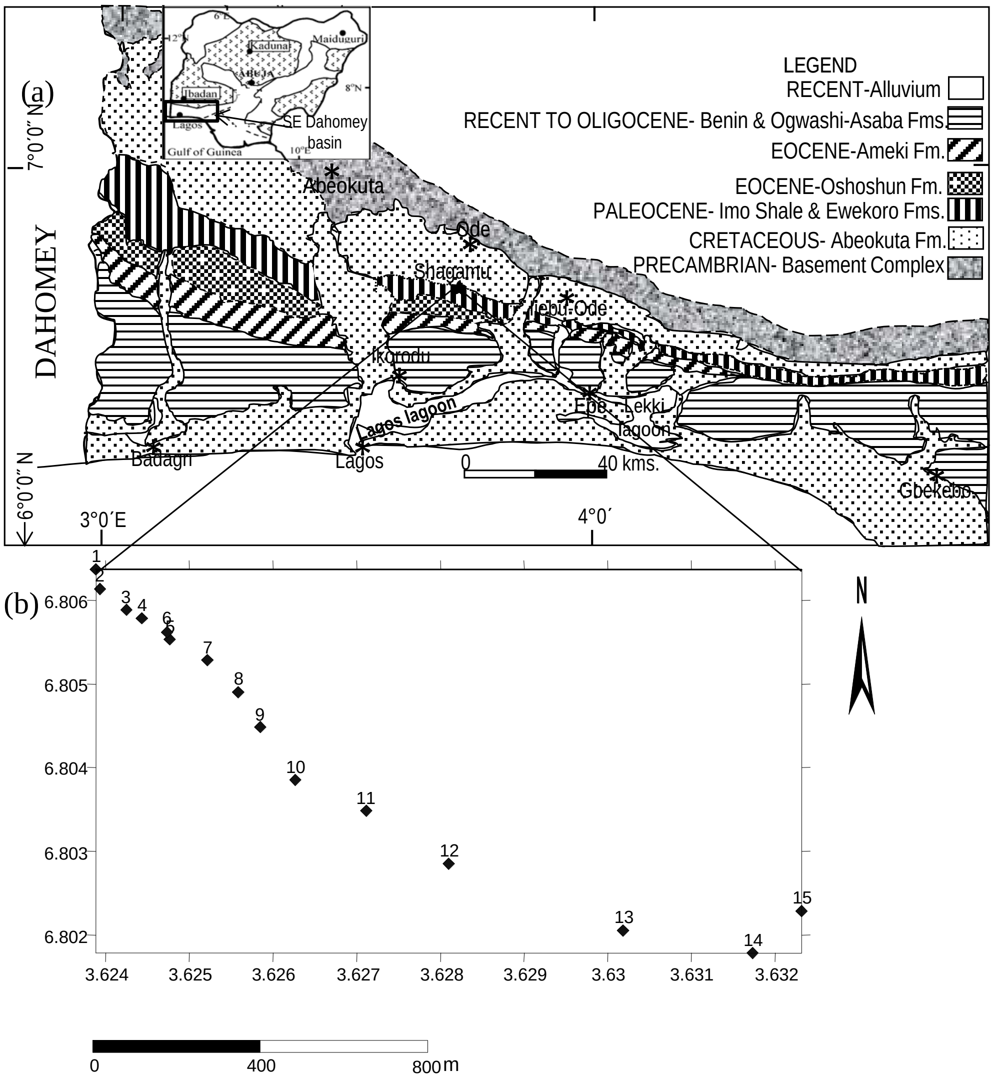

Figure 1. (a) Geological map of eastern Dahomey Embayment (redrawn after [11]; (b) Study area map with NW-SE trending sample locations.

Ewekoro Formation and; the shelly biomicrite and Algal biosparite upper unit [1]. It's of Paleocene age based on fossil evidence (foraminifera and ostracods) and deposited in a shallow marine environment [16] [17].

3. Materials and Methods

This work involved a geological field survey of the study area, a geochemical analysis and a computer-based geo-modelling to evaluate the CaO and SiO_2 distribution in the limestone formation. The field work entailed examination and logging of quarry sections at Shagamu and 83 representative samples were obtained for laboratory analysis. Sampling was done from bottom to top at distinct limestone beds in fifteen sections in a NW-SE traverse (**Figure 1(b)**) and readings of geographical location obtained using a GPS device.

Sample preparation and analysis were done in the field-based laboratory of West African Portland Cement, Shagamu. Samples were washed, air dried, ground to powder form and homogenized; thereafter 2 g of each sample was mixed with spectroflux powder and 0.6 g of $LiNO_3$ salt in an agate mortar. The mixture was poured into fusing containers on a burner within M4 fluxer equipment and switched on for fifteen minutes to produce fused pellets. Fused pellets produced were analyzed for major elements using an X-Ray fluorescence machine (ARL 9900 XP). Loss on ignition (LOI) was determined separately by calculating weight loss after heating 2 g of each sample in a furnace for 1 hour at 1000˚C.

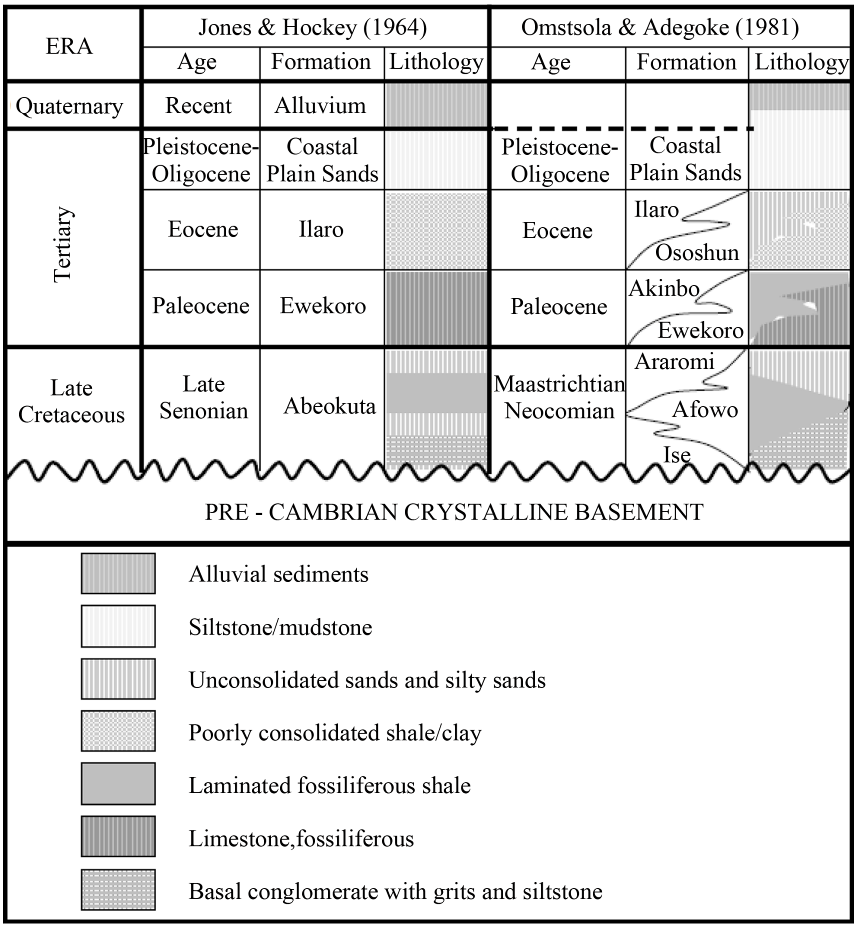

Figure 2. Stratigraphy of the Dahomey Embayment (After [2] and [9]).

The geochemical results obtained (**Table 1**) were further evaluated using a computer programme (*Surfer*^{TM}) to generate geochemical models for the distribution of CaO and SiO_2 (the main component and impurity in limestones respectively). To achieve this, the latitudinal and longitudinal readings were scaled to the X and Y-axes respectively, while the corresponding chemical concentrations (in wt%) of CaO and SiO_2 were scaled to the Z-axis for each of the beds. Through a statistical algorithm called *kriging*, the GPS readings and concentrations of CaO and SiO_2 were interpolated, resulting in a spatio-temporal distribution of these oxides within the various beds through a grid-based contouring of their concentrations. This variogram mathematically express the variance of the geochemical concentration in each of the beds giving a series of surface geochemical models that may constitute baseline information for further exploitation of the deposit.

4. Results and Interpretations

4.1. Field Relationships

Field study revealed five limestone beds, labeled E to A spanning the 15 sections logged (**Figure 1** and **Figure 3**); although a sixth bed, F (which is quite silty with large amount of quartz) was recognized belonging to the underlying Araromi Formation. Bed E is the oldest bed among the limestone units. It's a light brown sandy algal bed with fossils embedded in sparry calcite cement. Bed D is light brown, shelly biomicritic and inter-fingered Bed E which is more friable, sandy algal biosparite, with the cementing material mostly sparry calcite. Bed C is dark grey, calcareous unit that comprised algal biomicrite facies. Bed B is grayish to brown in colour, hard with greater tenacity than the overlying bed and comprised sandy algal biomicrite embedded in micrite cement. Bed A is a red phosphatic limestone (typifying the intra-sparite facies) that is crystalline textured with localized quartz fillings within vugs and caves induced by migrating acidic fluids.

Table 1. Major elements composition (wt%) of Limestones from the Ewekoro Formation exposed at Shagamu.

Bed Name	LOI (%)	SiO_2 (%)	Al_2O_3 (%)	Fe_2O_3 (%)	CaO (%)	MgO (%)	SO_3 (%)	K_2O (%)	Na_2O (%)	TiO_2 (%)	P_2O_5 (%)	MnO (%)	Cr_2O_3 (%)	Total (%)
Location 1														
Bed A1	44.89	00.88	0.98	0.61	52.01	0.62	0.18	0.04	00.00	0.01	0.08	0.04	0.00	100.3
Bed B1	44.52	01.98	1.59	1.28	48.78	0.83	0.92	0.06	00.00	0.03	0.30	0.02	0.00	100.3
Bed C1	44.52	01.98	1.59	1.28	48.78	0.81	0.47	0.06	00.00	0.08	0.12	0.01	0.00	100.7
Bed D1	41.67	01.85	0.52	0.62	54.22	0.64	0.15	0.06	00.20	0.03	0.04	0.01	0.00	100.0
Bed E1	40.38	05.22	0.55	1.42	49.98	2.26	0.15	0.06	00.00	0.04	0.06	0.04	0.00	100.2
Bed F1	42.17	09.15	2.44	1.33	42.84	1.40	0.64	0.08	00.00	0.10	0.17	0.02	0.00	100.4
Location 2														
Bed A2	42.05	01.40	1.07	0.86	53.97	0.72	0.29	0.03	00.00	0.01	0.08	0.04	0.00	100.5
Bed B2	43.69	01.10	0.95	0.54	52.85	0.78	0.24	0.05	00.00	0.02	0.09	0.01	0.00	100.3
Bed C2	37.70	10.65	1.63	1.72	46.73	0.87	0.92	0.13	00.00	0.15	0.25	0.01	0.00	100.8
Bed D2	40.25	05.34	0.55	0.64	52.70	0.64	0.10	0.06	00.20	0.02	0.04	0.01	0.00	100.6
Bed E2	40.25	06.34	1.96	1.82	46.33	3.15	0.42	0.08	00.00	0.13	0.11	0.04	0.00	100.6
Location 3														
Bed A3	41.56	01.51	0.90	0.67	54.24	1.24	0.39	0.02	00.00	0.01	0.08	0.04	0.00	100.7
Bed B3	43.90	01.57	0.63	1.01	50.05	3.31	0.17	0.05	00.00	0.03	0.03	0.01	0.00	100.8
Bed C3	29.93	22.15	3.04	3.06	38.81	3.14	0.74	0.25	00.00	0.27	0.27	0.01	0.00	100.7
Bed D3	31.14	31.21	1.64	1.05	34.22	0.62	0.23	0.07	00.00	0.06	0.24	0.03	0.00	100.5
Bed E3	40.25	06.34	1.96	1.82	46.33	3.15	0.42	0.08	00.00	0.13	0.11	0.04	0.00	100.6
Location 4														
Bed A4	43.29	01.15	0.53	0.67	52.75	1.72	0.30	0.03	00.00	0.01	0.09	0.01	0.00	100.6
Bed D4	31.79	27.58	1.57	1.24	37.05	0.74	0.21	0.07	10.00	0.11	0.20	0.03	0.00	100.6
Bed E4	43.83	02.58	1.23	0.83	50.48	0.75	0.78	0.04	10.00	0.04	0.10	0.01	0.00	100.7
Location 5														
Bed A5	43.29	01.15	0.53	0.67	52.70	1.72	0.30	0.03	00.00	0.01	0.09	0.02	0.00	100.2
Bed B5	43.93	01.57	0.63	1.01	50.04	3.31	0.17	0.05	00.00	0.03	0.02	0.01	0.00	100.8
Bed C5	31.14	22.23	3.07	3.43	36.84	2.05	0.82	0.28	00.00	0.20	0.34	0.01	0.00	100.4
Bed D5	32.79	26.58	1.57	1.24	37.06	0.74	0.21	0.07	00.00	0.11	0.24	0.01	0.00	100.6
Bed E5	43.81	02.58	1.23	0.83	50.49	0.75	0.78	0.04	00.00	0.04	0.10	0.01	0.00	100.6
Location 6														
Bed A6	40.92	02.07	1.73	0.68	52.58	1.03	0.77	0.06	00.00	0.00	0.22	0.05	0.00	100.1
Bed B6	45.10	01.26	1.64	0.51	50.01	1.01	0.31	0.05	00.00	0.02	0.10	0.01	0.00	100.0
Bed C6	31.14	22.23	3.07	3.43	35.84	2.05	0.82	0.28	00.00	0.20	0.34	0.02	0.00	99.42

Continued

Sample code	LOI (%)	SiO_2 (%)	Al_2O_3 (%)	Fe_2O_3 (%)	CaO (%)	MgO (%)	SO_3 (%)	K_2O (%)	Na_2O (%)	TiO_2 (%)	P_2O_5 (%)	MnO (%)	Cr_2O_3 (%)	Total (%)
Bed D6	33.79	25.58	1.57	1.24	37.08	0.74	0.21	0.07	00.00	0.11	0.24	0.02	0.00	100.7
Bed E6	43.83	02.58	1.23	0.83	50.48	0.75	0.78	0.04	00.00	0.04	0.10	0.01	0.00	100.6
Location 7														
Bed A7	40.92	02.07	1.73	0.68	52.57	1.03	0.77	0.06	00.00	0.00	0.22	0.02	0.00	100.1
Bed B7	45.20	01.26	1.64	0.51	50.20	1.01	0.31	0.05	00.00	0.02	0.10	0.01	0.00	100.3
Bed C7	32.14	21.23	3.07	3.43	36.84	2.05	0.82	0.28	00.00	0.20	0.34	0.02	0.00	100.1
Bed D7	31.79	27.58	1.57	1.24	37.09	0.74	0.21	0.07	00.00	0.11	0.24	0.01	0.00	100.7
Bed E7	43.83	02.55	1.23	0.83	50.45	0.75	0.78	0.04	00.00	0.04	0.10	0.01	0.00	100.6
Bed F7	42.17	09.15	2.44	1.33	42.84	1.40	0.64	0.08	00.00	0.10	0.17	0.01	0.00	100.3
Location 8														
Bed A8	42.09	01.30	0.47	0.55	55.08	0.93	0.16	0.03	00.00	0.02	0.10	0.01	0.00	100.7
Bed B8	41.30	01.40	0.81	0.83	54.13	0.61	0.44	0.07	00.34	0.02	0.04	0.01	0.00	100.0
Bed C8	42.17	09.15	2.44	1.33	42.84	1.40	0.64	0.08	00.00	0.10	0.17	0.01	0.00	100.3
Bed D8	30.79	27.58	1.57	1.24	37.12	0.74	0.21	0.07	00.00	0.11	0.24	0.02	0.00	99.69
Bed E8	43.83	02.54	1.23	0.83	50.46	0.75	0.78	0.04	00.00	0.04	0.10	0.01	0.00	100.6
Bed F8	42.17	09.15	2.44	1.33	42.84	1.40	0.64	0.08	00.00	0.10	0.17	0.01	0.00	100.3
Location 9														
Bed A9	43.19	00.47	0.37	0.88	54.20	0.39	0.21	0.02	0.00	0.01	0.92	0.05	0.00	100.7
Bed B9	33.58	09.98	1.53	3.34	48.19	0.73	2.27	0.17	0.00	0.15	0.70	0.01	0.00	100.7
Bed C9	36.41	09.91	1.84	1.72	49.17	0.88	1.24	0.11	0.00	0.11	0.28	0.01	0.00	100.7
Bed D9	31.80	27.58	1.57	1.24	37.05	0.74	0.21	0.07	0.00	0.11	0.24	0.01	0.00	100.6
Bed E9	43.83	02.59	1.23	0.83	50.49	0.75	0.78	0.04	0.00	0.04	0.10	0.01	0.00	100.7
Bed F9	42.17	09.15	2.44	1.33	42.84	1.40	0.64	0.08	0.00	0.10	0.17	0.01	0.00	100.3
Location 10														
Bed A10	41.68	01.24	0.32	0.67	55.77	0.79	0.13	0.02	0.00	0.02	0.03	0.03	0.00	100.7
Bed B10	36.63	01.56	0.56	0.92	59.99	0.68	0.30	0.05	0.00	0.03	0.05	0.01	0.00	100.8
Bed C10	36.51	09.91	1.84	1.72	48.17	0.88	1.24	0.11	0.00	0.11	0.28	0.04	0.00	100.7
Bed D10	43.42	01.69	0.78	0.96	52.70	0.52	0.15	0.05	0.00	0.03	0.06	0.02	0.00	100.4
Bed E10	43.83	02.58	1.23	0.83	50.48	0.75	0.78	0.04	0.00	0.04	0.10	0.01	0.00	100.7
Bed F10	17.64	45.18	1.22	1.62	33.71	0.11	0.16	0.12	0.00	0.09	0.22	0.02	0.00	100.1
Location 11														
Bed A11	41.68	01.24	0.32	0.67	55.75	0.79	0.13	0.02	0.00	0.02	0.03	0.01	0.00	100.7
Bed B11	38.47	02.94	0.94	0.94	55.08	0.62	0.69	0.07	0.16	0.06	0.04	0.01	0.00	100.0

Continued

Bed C11	42.53	07.58	1.63	1.36	45.29	0.87	1.00	0.09	0.00	0.10	0.25	0.01	0.00	100.7
Bed D11	36.41	09.91	1.84	1.72	48.19	0.88	1.24	0.11	0.00	0.11	0.28	0.01	0.00	100.7
Bed E11	37.32	01.68	0.93	0.67	53.30	0.72	0.20	0.05	0.00	0.02	0.09	0.03	0.00	100.1
Bed F11	17.64	45.18	1.22	1.62	33.71	0.11	0.16	0.12	0.00	0.09	0.22	0.02	0.00	100.1
Location 12														
Bed A12	41.68	01.24	0.32	0.67	55.76	0.79	0.13	0.02	0.00	0.02	0.03	0.01	0.00	100.7
Bed B12	41.66	01.85	0.72	0.58	54.65	0.64	0.30	0.05	0.00	0.03	0.15	0.00	0.00	100.6
Bed C12	24.31	16.02	4.04	2.64	50.78	1.14	0.77	0.14	0.00	0.23	0.22	0.03	0.00	100.3
Bed D12	35.41	09.91	1.84	1.72	48.20	0.88	1.24	0.11	0.00	0.11	0.28	0.02	0.00	99.72
Bed E12	37.32	01.69	0.93	0.67	53.37	0.72	0.20	0.05	0.00	0.02	0.09	0.03	0.00	100.0
Bed F12	17.64	45.18	1.22	1.62	33.71	0.11	0.16	0.12	0.00	0.09	0.22	0.03	0.00	100.1
Location 13														
Bed A13	43.99	00.79	0.76	0.63	53.54	0.50	0.16	0.02	0.00	0.01	0.10	0.05	0.00	100.6
Bed B13	42.74	01.27	0.45	0.75	54.42	0.63	0.21	0.04	0.00	0.02	0.07	0.00	0.00	100.6
Bed C13	37.09	03.51	1.00	1.05	56.52	1.02	0.41	0.04	0.00	0.06	0.06	0.00	0.00	100.8
Bed D13	36.41	09.91	1.84	1.72	48.18	0.88	1.24	0.11	0.00	0.11	0.28	0.00	0.00	100.7
Bed E13	42.59	01.69	0.93	0.67	53.39	0.72	0.20	0.05	0.00	0.02	0.09	0.01	0.00	100.4
Bed F13	17.64	45.18	1.22	1.62	33.71	0.11	0.16	0.12	0.00	0.09	0.22	0.02	0.00	100.1
Location 14														
Bed A14	42.82	01.70	1.24	0.75	52.72	0.65	0.28	0.03	0.00	0.01	0.21	0.06	0.00	100.4
Bed B14	41.50	02.27	0.79	0.70	53.77	0.89	0.54	0.06	0.00	0.03	0.17	0.00	0.00	100.7
Bed C14	32.06	21.92	2.79	3.09	38.61	0.79	1.27	0.28	0.00	0.26	0.50	0.01	0.00	100.6
Bed D14	35.41	09.91	1.84	1.72	48.37	0.88	1.24	0.11	0.00	0.11	0.28	0.02	0.00	99.89
Bed E14	43.58	01.69	0.93	0.67	53.34	0.72	0.20	0.05	0.00	0.02	0.09	0.01	0.00	100.3
Bed F14	17.64	45.18	1.22	1.62	33.71	0.11	0.16	0.12	0.00	0.09	0.22	0.01	0.00	100.1
Location 15														
Bed A15	42.82	01.70	1.24	0.75	52.71	0.65	0.28	0.03	0.00	0.01	0.21	0.06	0.00	100.4
Bed B15	43.90	01.12	0.72	1.52	50.74	2.33	0.16	0.04	0.00	0.02	0.03	0.02	0.00	100.6
Bed C15	33.06	21.92	2.79	3.09	36.61	0.79	1.27	0.28	0.00	0.26	0.50	0.01	0.00	100.6
Bed D15	36.31	09.91	1.84	1.72	48.17	0.88	1.24	0.11	0.00	0.11	0.28	0.01	0.00	100.6
Bed E15	42.58	01.69	0.93	0.67	53.38	0.72	0.20	0.05	0.00	0.02	0.09	0.01	0.00	100.4
Bed F15	17.64	45.18	1.22	1.62	33.71	0.11	0.16	0.12	0.00	0.09	0.22	0.02	0.00	100.1

4.2. Major Elements Distribution

The concentrations (in wt% of oxides) of major elements in the limestone samples are shown in **Table 1**. The

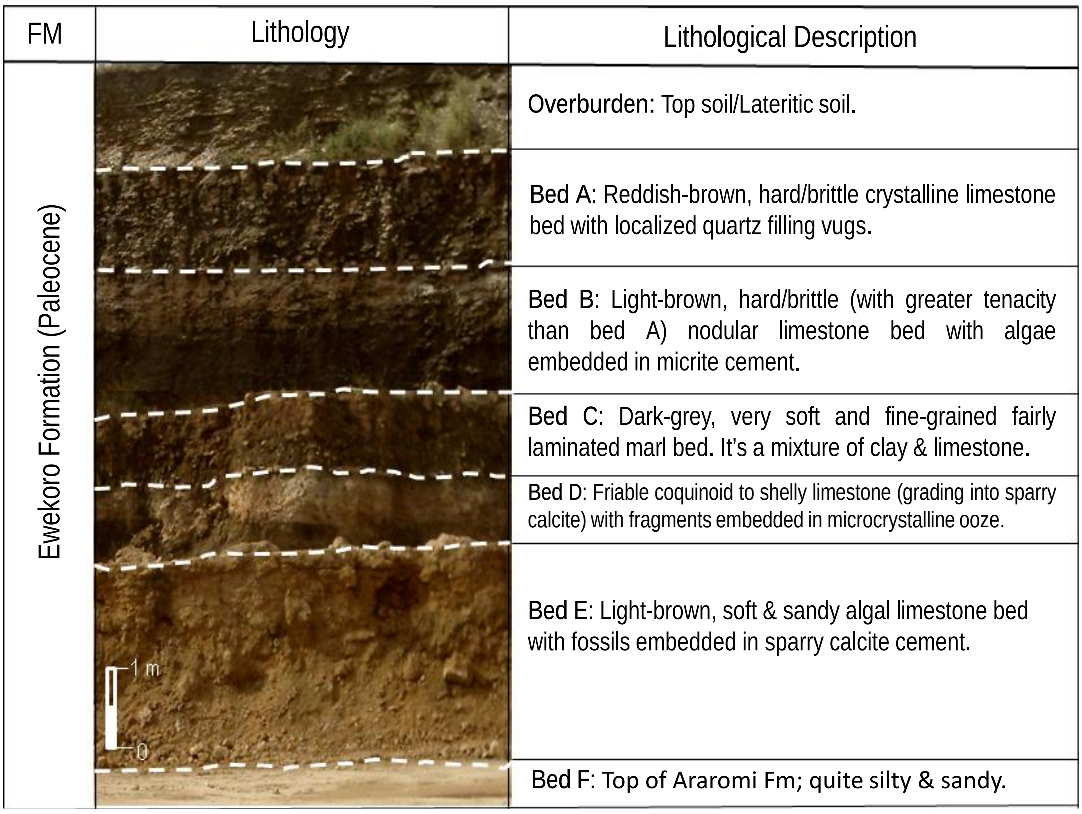

Figure 3. A representative lithologic section of the Ewekoro Formation (Fm) observed at Shagamu Quarry.

limestone samples analyzed are enriched (>1 wt%) in CaO (33.7 - 59.99 wt%, average 47.29 wt%) and slightly depleted to enriched in SiO_2 (0.47 - 31.21 wt%), Al_2O_3 (0.47 - 3.23 wt%), MgO (0.39 - 3.15 wt%), Fe_2O_3 (0.51 - 3.43 wt%) and SO_3 (0.10 - 2.27 wt%). However, they are depleted (<1 wt%) in the alkalis (Na_2O and K_2O), TiO_2, MnO, P_2O_5 and Cr_2O_3. LOI varies between 17.64 - 45.10 wt percent. The values of CaO and MgO tend to decrease down the Formation with increasing silica content probably due to the presence of non-carbonate input transported from adjacent continental sources.

4.3. CaO and SiO_2 Variations in the Ewekoro Limestone Formation

A marked inverse negative correlation exists between SiO_2 and CaO contents of the limestones (**Figure 4**). A generalized geochemical variation model for the area representing the SiO_2 distribution is depicted in **Figure 5**. A bed-by-bed spatio-temporal geochemical distribution of the concentrations of CaO and SiO_2 is discussed below in super-positional order.

4.3.1. CaO and SiO_2 Variation in Bed E

Bed E is 1 - 2 m thick, occurring at depths of 17 - 38 m and 18 - 40 m at the upper and lower surfaces respectively. **Table 1** shows that CaO content ranged from 46.33 - 53.39 wt%, while SiO_2 ranged from 1.68 to 6.34 wt%. **Figure 6** is the 2-D and 3-D model views of CaO and SiO_2. A reduction in CaO concentration was noticed mostly in the south-central and northwestern part of the study area. However, an average abundance of CaO (>50 wt%) was maintained in other portions of the bed keeping SiO_2 proportions at minima level.

This zone carries the highest concentration and purest form of calcite. These calcite-rich zones could serve as suitable targets for limestone mining works, development and the production of Portland cement.

4.3.2. CaO and SiO_2 Variation in Bed D

Bed D is ≈3 - 4 m thick and occurred at depths of 14 - 34 m and 17 - 38 m at the upper and lower surfaces respectively. From **Table 1**, the CaO contents ranged from 34.22 - 54.22 wt%, while SiO_2 ranged from 1.69 - 31.21 wt%.

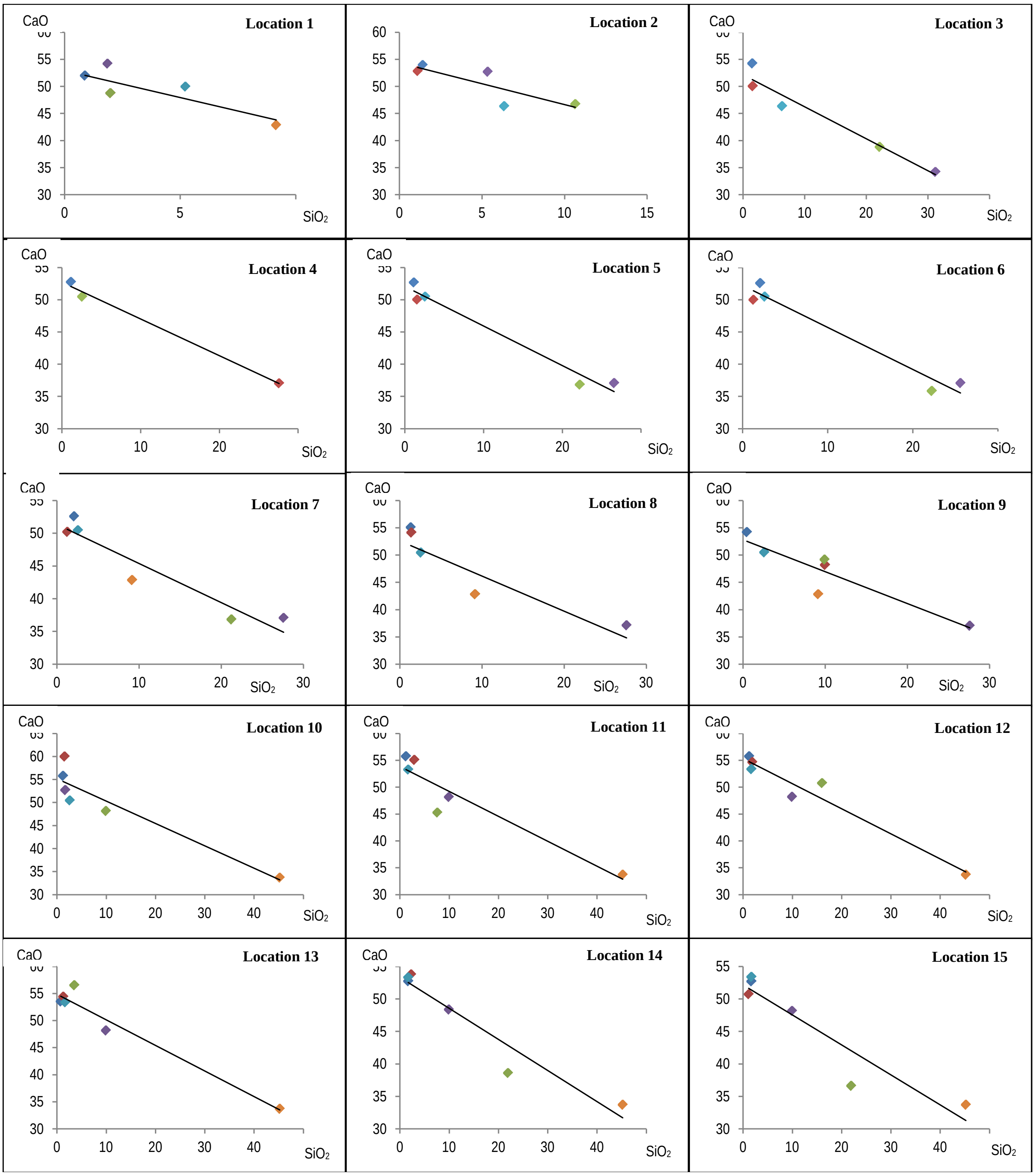

Figure 4. SiO_2 (in wt%) versus CaO (in wt%) plots revealing a marked inverse relationship.

A 2-D and 3-D model views of CaO and SiO_2 concentration is shown in **Figure 7**. Peaks of CaO and SiO_2 concentrations were recorded in the southwestern and northwestern flanks respectively. Again, just as in bed E for a decline in CaO concentration there is a corresponding abundance of SiO_2 was observed.

4.3.3. CaO and SiO_2 Variation in Bed C

This bed is 3.5 m thick occupied depths of 8.6 - 9.3 m and 20.2 - 23.7 m at the upper and lower surfaces respectively. **Table 1** showed CaO concentration of 35.84 - 56.52 wt%, while SiO_2 is 1.98 - 22.23 wt%. Geochemical variation models of CaO and SiO_2 indicated a decline in CaO (with small peaks in southern part) concentration

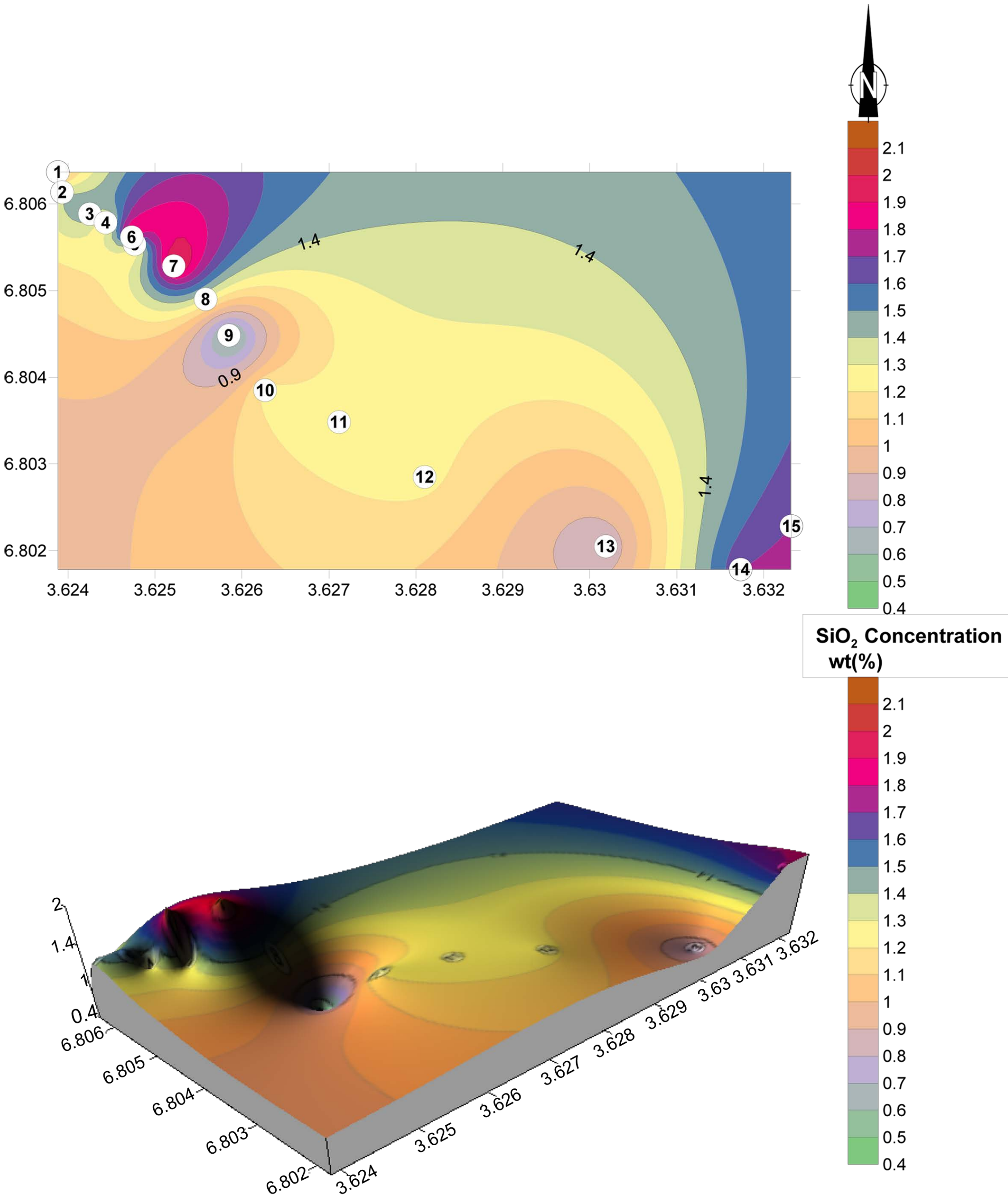

Figure 5. A generalized SiO_2 (in wt%) distribution models of the study area.

with an accompanying enrichment in SiO_2 at both the southeastern and northwestern ends of the study area (**Figure 8**).

4.3.4. CaO and SiO_2 Variation in Bed B

This 3 - 5 m thick bed occupied a depth of 7 - 25 m and 10 - 30 m at the upper and lower bedding planes respectively.

SiO_2 content is 1.10 - 9.98 wt% and CaO is 48.19 - 59.99 wt% (**Table 1**). **Figure 9** is the 2-D and 3-D model views of the bed B, indicating a uniformly high CaO concentration with a sharp drop in the mid-western part. SiO_2 concentration is very low in this bed; a peak concentration apparent in the mid-western part coincided with

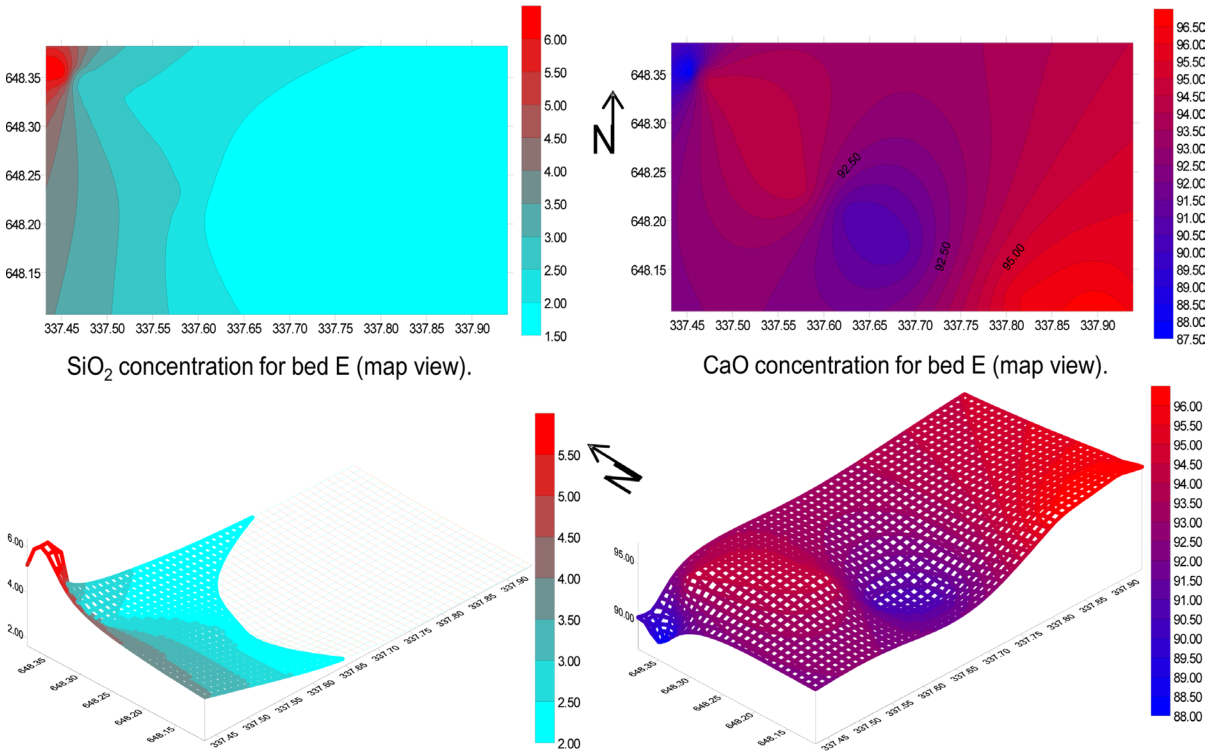

SiO_2 concentration for bed E (map view). CaO concentration for bed E (map view).

SiO_2 concentration for bed E (3-D view). CaO concentration for bed E (3-D view).

Figure 6. Geochemical variation models of SiO_2 (in wt%) and CaO (in wt%) for bed E.

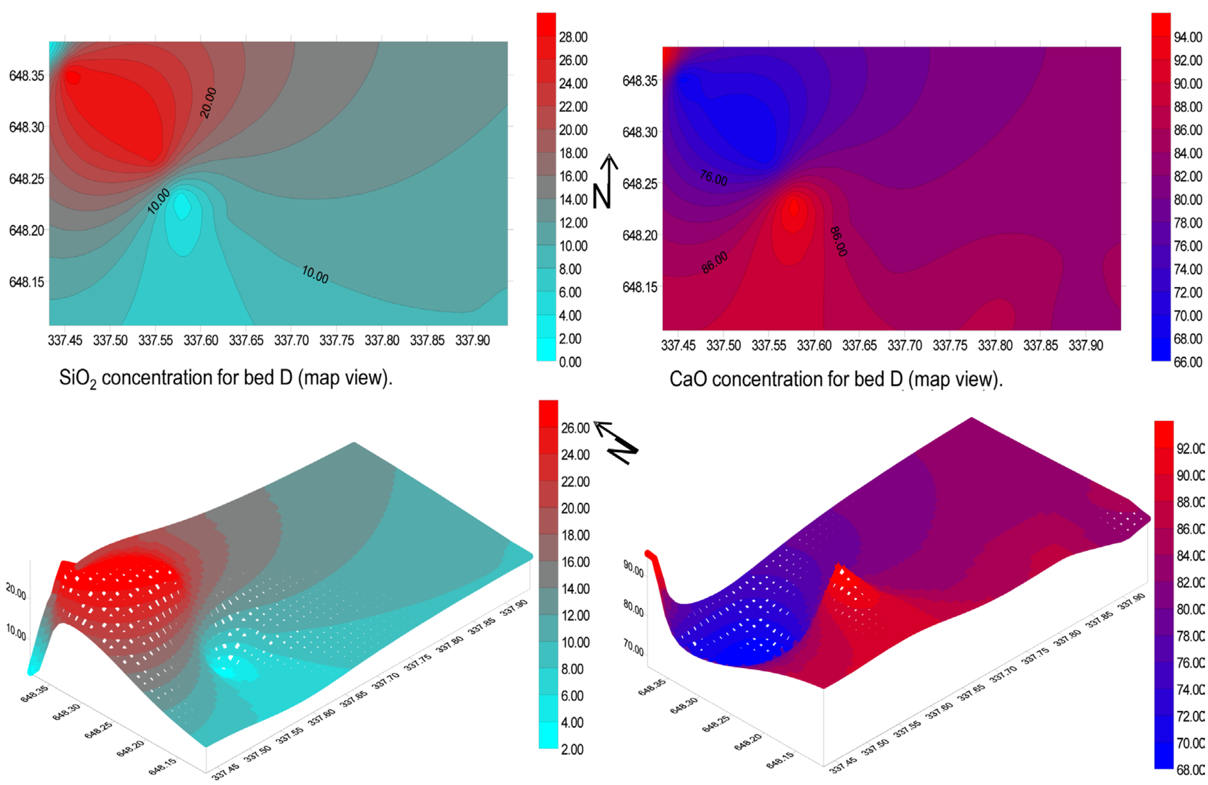

SiO_2 concentration for bed D (map view). CaO concentration for bed D (map view).

SiO_2 concentration for bed D (3-D view). CaO concentration for bed D (3-D view).

Figure 7. Geochemical variation models of SiO_2 (in wt %) and CaO (in wt%) for bed D.

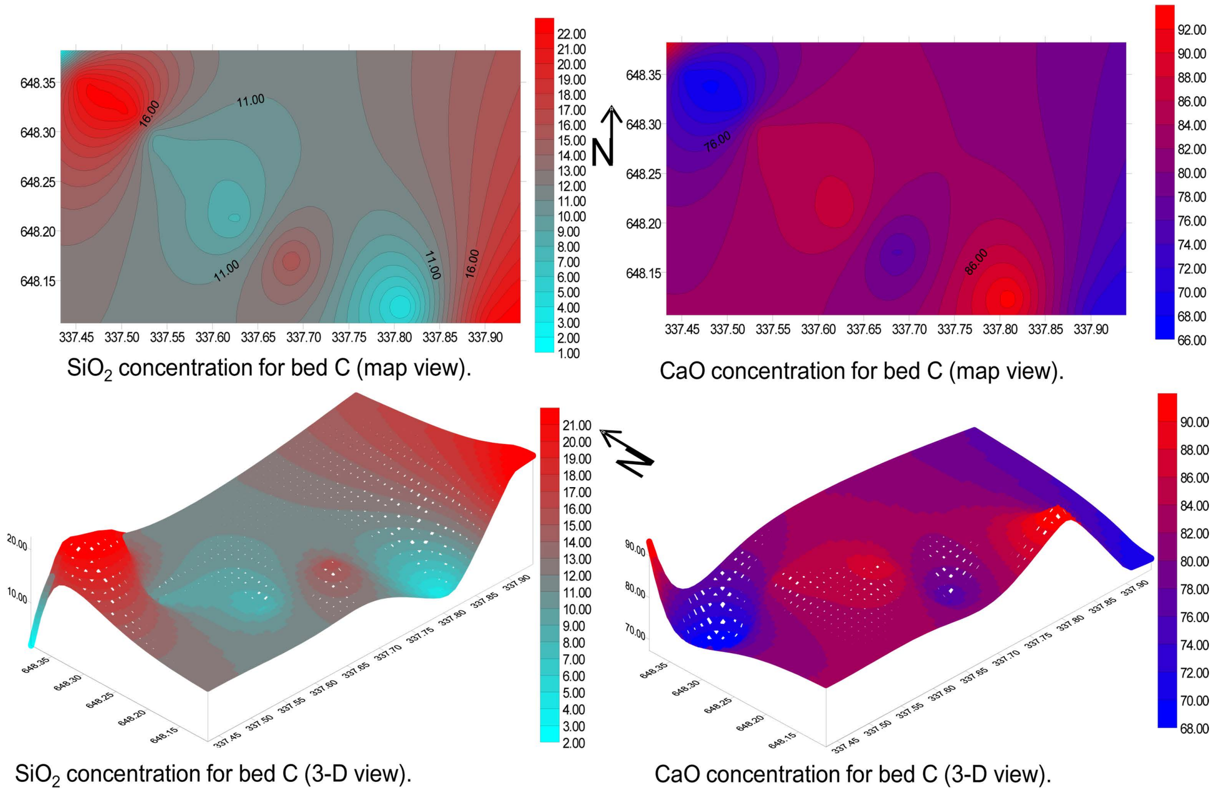

Figure 8. Geochemical variation models of SiO_2 (in wt%) and CaO (in wt%) for bed C.

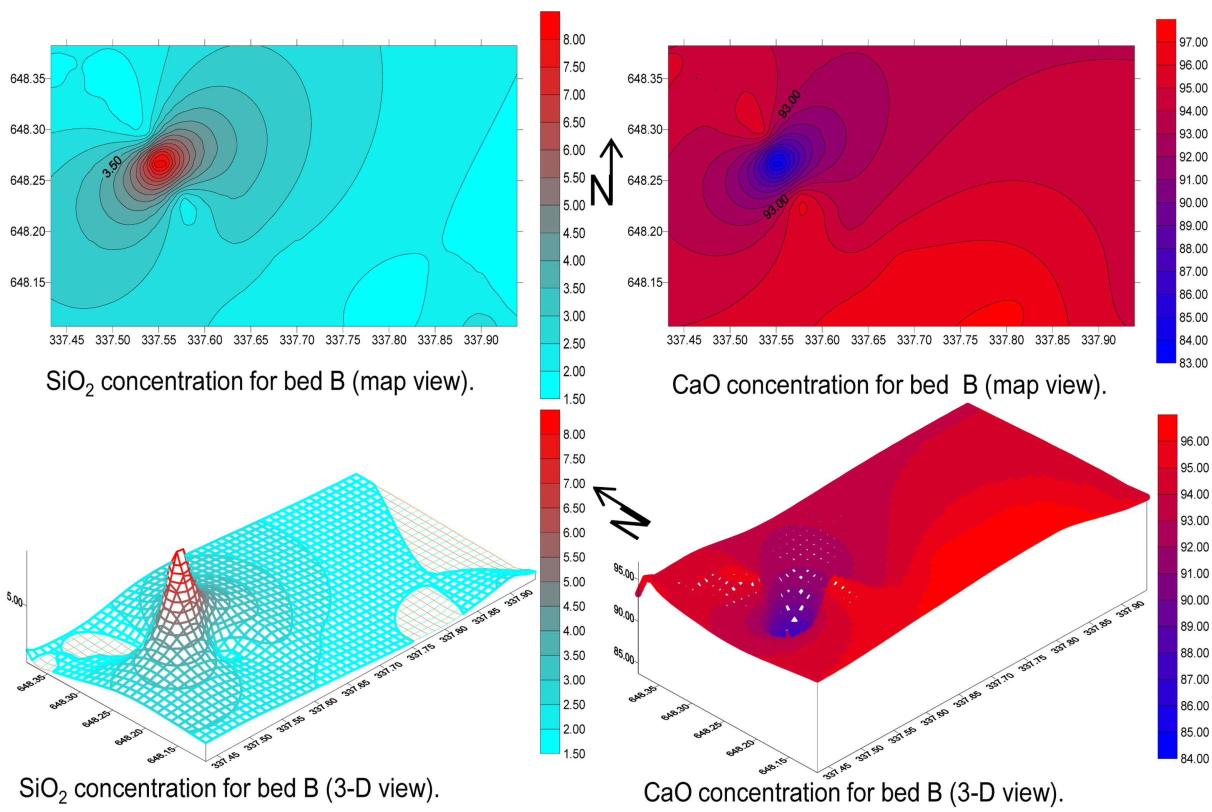

Figure 9. Geochemical variation models of SiO_2 (in wt%) and CaO (in wt%) for bed B.

the CaO lowest concentration. A notable increase in CaO concentration was noticed in compensation for the decline in SiO_2 concentration, a trend similar to that of the aforementioned beds.

4.3.5. CaO and SiO_2 Variation in Bed A

This bed is ≈5 m thick, occurring at depth range of 5 - 25 m. For this bed, CaO content is 52.01 - 55.77 wt% while SiO_2 is 0.47 - 2.07 wt% (**Table 1**). **Figure 10** is the geochemical model for bed A in 2-D and 3-D views respectively. From this model, CaO indicated a peak concentration in the southwestern part, while SiO_2 showed a high concentration running almost diagonally from the NNW part to the SSE part. This is shown by the corresponding "trough" on the model as against the "crests" of high CaO concentration.

5. Discussion

5.1. Geochemistry, Provenance and Depositional Environment

The silica content varies widely (0.47 - 3.21 wt%, **Table 1**); an indication that the adjacent basement complex rocks of southwestern Nigeria may have sourced varied amounts of these detrital impurity and/or its dissolved component in the shallow marine environment. Geochemical plots (**Figure 4**) of SiO_2 against CaO for all the samples analyzed clearly revealed a similar and unique trend marked by increase in CaO with corresponding decrease in SiO_2 contents and vice versa. This SiO_2-CaO negative correlation can be attributed to chemical diagenetic replacement. At the shallow part of the upper continental crust where silica is readily made available through weathering and erosion, calcite reacts with it to form a calc-silicate at low temperature and pressure. Also, at all stages of diagenesis, dissolved silica (derived from dissolution of siliceous tests of marine organisms) replaces calcite. Fluvial silica input often augment dissolved silica in the basin at the unset of shallow marine condition. However, $CaCO_3$ production dominates as shallow marine conditions become fully established and silica supply from the hinterland reduces. Hence the higher the SiO_2 input, the more the continental influence, whereas the $CaCO_3$ production signals shallow marine incursion.

The low alumina content confirms a low index of weathering of the alumino-silicates such as feldspars and micas in the adjacent basement areas during transportation and deposition prior to diagenesis [18]. Fe_2O_3 is usually

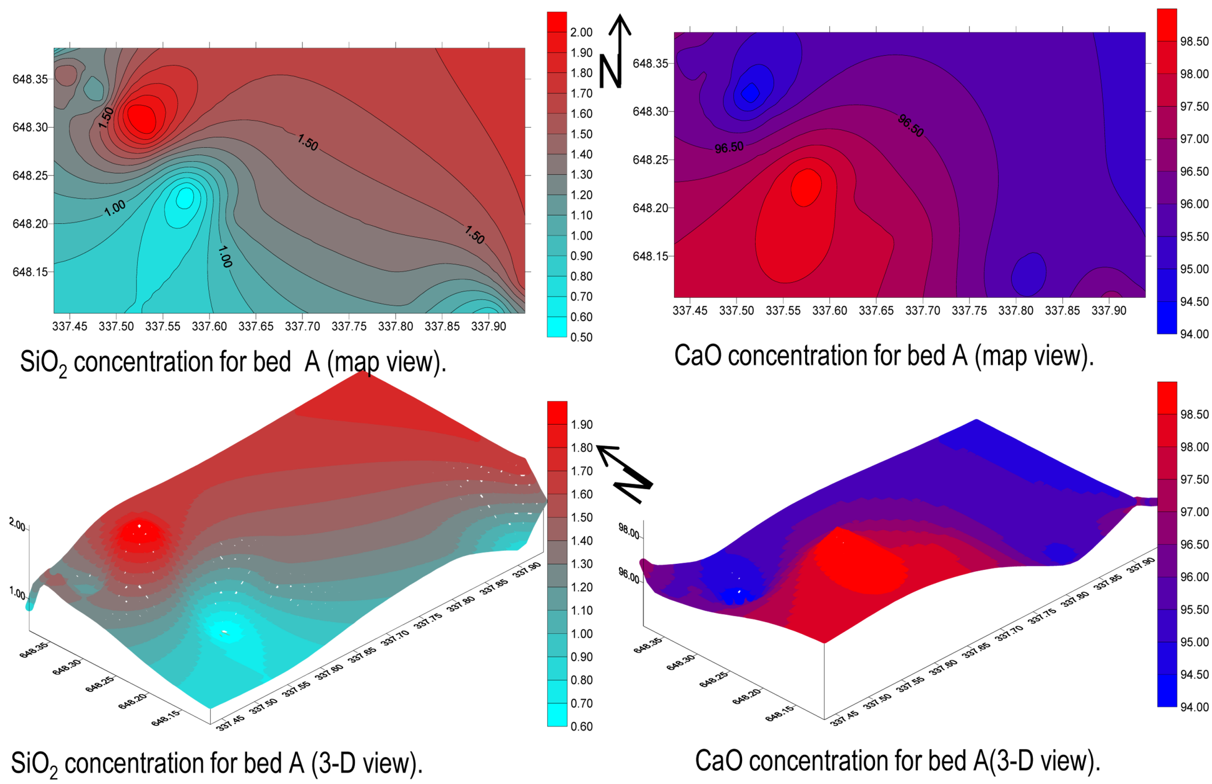

Figure 10. Geochemical variation models of SiO_2 (in wt%) and CaO (in wt%) for bed A.

Table 2. Classification of calcium and magnesium contents of the Ewekoro limestone (After Todd [19]).

Sample code	CaO (wt%)	MgO (wt%)	Standard ratio Ca/Mg	Reciprocal ratio Mg/Ca	Descriptive term
Bed A1	52.01	0.62	83.88	0.011	Limestone
Bed B1	48.78	0.83	58.77	0.017	Limestone
Bed C1	48.78	0.81	60.22	0.016	Limestone
Bed D1	54.22	0.64	84.71	0.011	Limestone
Bed E1	49.98	2.26	22.11	0.045	Magnesian limestone
Bed F1	42.84	1.4	30.60	0.032	Magnesian limestone
Bed A2	53.97	0.72	74.95	0.013	Limestone
Bed B2	52.85	0.78	67.75	0.014	Limestone
Bed C2	46.73	0.87	53.71	0.018	Limestone
Bed D2	52.7	0.64	82.34	0.012	Limestone
Bed E2	46.33	3.15	14.70	0.067	Magnesian limestone
Bed A3	54.24	1.24	43.74	0.022	Limestone
Bed B3	50.05	3.31	15.12	0.066	Magnesian limestone
Bed C3	38.81	3.14	12.35	0.080	Dolomitic limestone
Bed D3	34.22	0.62	55.19	0.018	Limestone
Bed E3	46.33	3.15	14.70	0.067	Magnesian limestone
Bed A4	52.75	1.72	30.66	0.032	Magnesian limestone
Bed D4	37.05	0.74	50.06	0.019	Limestone
Bed E4	50.48	0.75	67.30	0.014	Limestone
Bed A5	52.7	1.72	30.63	0.032	Magnesian limestone
Bed B5	50.04	3.31	15.11	0.066	Magnesian limestone
Bed C5	36.84	2.05	17.97	0.055	Magnesian limestone
Bed D5	37.06	0.74	50.08	0.019	Limestone
Bed E5	50.49	0.75	67.32	0.014	Limestone
Bed A6	52.58	1.03	51.04	0.019	Limestone
Bed B6	50.01	1.01	49.51	0.020	Limestone
Bed C6	35.84	2.05	17.48	0.057	Magnesian limestone
Bed D6	37.08	0.74	50.10	0.019	Limestone
Bed E6	50.48	0.75	67.30	0.014	Limestone
Bed A7	52.57	1.03	51.03	0.019	Limestone
Bed B7	50.2	1.01	49.70	0.020	Limestone
Bed C7	36.84	2.05	17.97	0.055	Magnesian limestone
Bed D7	37.09	0.74	50.12	0.019	Limestone
Bed E7	50.45	0.75	67.26	0.014	Limestone
Bed F7	42.84	1.4	30.60	0.032	Magnesian limestone

Continued

Sample code	CaO (wt%)	MgO (wt%)	Standard ratio Ca/Mg	Reciprocal ratio Mg/Ca	Descriptive term
Bed A8	55.08	0.93	59.22	0.016	Limestone
Bed B8	54.13	0.61	88.73	0.011	Limestone
Bed C8	42.84	1.4	30.60	0.032	Magnesian limestone
Bed D8	37.12	0.74	50.16	0.019	Limestone
Bed E8	50.46	0.75	67.28	0.014	Limestone
Bed F8	42.84	1.4	30.60	0.032	Magnesian limestone
Bed A1	52.01	0.62	83.88	0.011	Limestone
Bed B1	48.78	0.83	58.77	0.017	Limestone
Bed C1	48.78	0.81	60.22	0.016	Limestone
Bed D1	54.22	0.64	84.71	0.011	Limestone
Bed E1	49.98	2.26	22.11	0.045	Magnesian limestone
Bed F1	42.84	1.4	30.60	0.032	Magnesian limestone
Bed A2	53.97	0.72	74.95	0.013	Limestone
Bed B2	52.85	0.78	67.75	0.014	Limestone
Bed C2	46.73	0.87	53.71	0.018	Limestone
Bed D2	52.7	0.64	82.34	0.012	Limestone
Bed E2	46.33	3.15	14.70	0.067	Magnesian limestone
Bed A3	54.24	1.24	43.74	0.022	Limestone
Bed B3	50.05	3.31	15.12	0.066	Magnesian limestone
Bed C3	38.81	3.14	12.35	0.080	Dolomitic limestone
Bed D3	34.22	0.62	55.19	0.018	Limestone
Bed E3	46.33	3.15	14.70	0.067	Magnesian limestone
Bed A4	52.75	1.72	30.66	0.032	Magnesian limestone
Bed D4	37.05	0.74	50.06	0.019	Limestone
Bed E4	50.48	0.75	67.30	0.014	Limestone
Bed A5	52.7	1.72	30.63	0.032	Magnesian limestone
Bed B5	50.04	3.31	15.11	0.066	Magnesian limestone
Bed C5	36.84	2.05	17.97	0.055	Magnesian limestone
Bed D5	37.06	0.74	50.08	0.019	Limestone
Bed E5	50.49	0.75	67.32	0.014	Limestone
Bed A6	52.58	1.03	51.04	0.019	Limestone
Bed B6	50.01	1.01	49.51	0.020	Limestone
Bed C6	35.84	2.05	17.48	0.057	Magnesian limestone
Bed D6	37.08	0.74	50.10	0.019	Limestone
Bed E6	50.48	0.75	67.30	0.014	Limestone
Bed A7	52.57	1.03	51.03	0.019	Limestone

Continued

Bed B7	50.2	1.01	49.70	0.020	Limestone
Bed C7	36.84	2.05	17.97	0.055	Magnesian limestone
Bed D7	37.09	0.74	50.12	0.019	Limestone
Bed E7	50.45	0.75	67.26	0.014	Limestone
Bed F7	42.84	1.4	30.60	0.032	Magnesian limestone
Bed A8	55.08	0.93	59.22	0.016	Limestone
Bed B8	54.13	0.61	88.73	0.011	Limestone
Bed C8	42.84	1.4	30.60	0.032	Magnesian limestone
Bed D8	37.12	0.74	50.16	0.019	Limestone
Bed E8	50.46	0.75	67.28	0.014	Limestone
Bed F8	42.84	1.4	30.60	0.032	Magnesian limestone

derived from intense chemical weathering of heavy mineral such as the ferromagnesians. Its low value indicates that the environment of deposition is a reducing one that does not favour the precipitation of Iron (II) to Iron (III) and thus leached away [18]. SO_3 is low probably because anoxic conditions prevailed in such quiet, low energy environments and there is rapid rate of sulphate reduction.

5.2. Implications of Ca/Mg and Mg/Ca Ratios for Palaeo-Salinity

Todd [19] presented a petrogenetic classification of carbonate rocks that involved the standard ratio, Ca/Mg and reciprocal ratio, Mg/Ca. The class limits of the standard ratio, Ca/Mg are: > 100 - 39.0, 39.0 - 12.3, 12.3 - 5.67, 5.67 - 1.86, 1.86 - 1.50, 1.50 - 1.22, and 1.22 - 1.00 expressed as limestone, magnesian limestone, dolomitic limestone, dolomitized limestone, calcareous dolomite, dolomite and magnesian dolomite respectively. Also, the class limits of the reciprocal ratio, Mg/Ca are: 0 - 0.03, 0.03 - 0.08, 0.08 - 0.18, 0.18 - 0.54, 0.54 - 0.67, 0.67 - 0.82 and 0.82 - 1.00 also expressed as limestone, magnesian limestone, dolomitic limestone, dolomitized limestone, calcareous dolomite, dolomite and magnesian dolomite respectively. The standard and reciprocal ratios of Ca and Mg composition of the Ewekoro limestone are shown in **Table 2**. More than 79% of the samples are classified as "pure" limestone and about 20% are magnesian limestone according to the method of [19]. The Ca/Mg ratio has implications for the stability conditions of the depositional environment that led to the formation of the carbonate(s) [20]. Naturally, the Mg/Ca ratio increases during evaporation of sea water, especially under saline environmental conditions. Considering the Ca/Mg and Mg/Ca ratios (**Table 2**) it can be concluded that the relative rate of evaporation of sea water and the palaeo-salinity condition was low, as such limestone was deposited more at the expense of dolomite. However, intermittent increase in rate of sea water evaporation and salinity resulted to the deposition of the few magnesian limestones.

6. Conclusion

The geochemical characterization of the limestones of the Ewekoro Formation through XRF analysis shed light on the level of chemical purity, provenance, diagenesis and environment of deposition of the study area. Geochemical variation model of SiO_2 and CaO showed a general distribution of purity level of the limestone that is applicable to mining operations. The limestone is rich in $CaCO_3$ with varied inputs of other oxides like SiO_2, MgO, Fe_2O_3, etc. A negative correlation resulted from SiO_2 against CaO plots implying replacement chemical diagenesis under a shallow marine setting. Ratios of Ca/Mg and Mg/Ca revealed relatively low sea water evaporation and palaeo-salinity conditions that encouraged $CaCO_3$ precipitation. However, occasional rise in sea water evaporation and salinity levels resulted in the formation of magnesian limestones.

Acknowledgements

The authors wish to acknowledge the Management of West African Portland Cement, Shagamu for permission to obtain samples and analyzing them.

References

[1] Nwajide, C.S. (2013) Geology of Nigeria's Sedimentary Basins. CSS Bookshop Ltd., Lagos.

[2] Jones, H.A. and Hockey, R.D. (1964) The Geology of Part of Southwestern Nigeria. *Geological Survey of Nigeria Bulletin*, **31**, 1-101.

[3] Reyment, R.A. (1965) Aspects of the Geology of Nigeria. Ibadan University Press, Ibadan.

[4] Elueze, A.A. and Nton, M.E. (2004) Organic Geochemical Appraisal of Limestones and Shales in Part of Eastern Dahomey Basin, Southwestern Nigeria. *Journal of Mining and Geology*, **40**, 29-40. http://dx.doi.org/10.4314/jmg.v40i1.18806

[5] Akinmonsin, A.A., Odewande and Akintola, A.I. (2005) Geochemical Composition and Textural Features of Some Carbonate Rocks in Parts of Southwestern Nigeria. *Ife Journal of Science*, **7**, 101-111.

[6] Ajayi, T.R., Oyawale, A.A., Islander, F.Y., Asubiojo, O.I., Klein, D.E. and Adediran, A.I. (2006) Trace and Rare Earth Elements Geochemistry of Oshosun Sediments of Dahomey Basin, Southwestern Nigeria. *Journal of Applied Science*, **6**, 2067-2076. http://dx.doi.org/10.3923/jas.2006.2067.2076

[7] Ofulume, A.B. (2012) Using Geochemical Criteria to Check the Depositional Environments Derived from Fossil Content and Microfacies of Shagamu, Mfamosing and Gboko Limestones, Nigeria. *Journal of Applied Science Research*, **8**, 371-376.

[8] Ogbe, F.G.A. (1972) Stratigraphy of Strata Exposed in Ewekoro Quarry, Western Nigeria. In: Dessauvagie, T.F.J. and Whiteman, A.J., Eds., *African Geology*, University of Ibadan Press, Ibadan, 305-322.

[9] Omatsola, M.E. and Adegoke, O.S. (1981) Tectonic Evolution and Cretaceous Stratigraphy of the Dahomey Basin. *Journal of Mining and Geology*, **18**, 130-137.

[10] Kingston, D.R., Dishroon, C.P. and Williams, P.A. (1983) Global Basin Classification System. *American Association of Petroleum Geologist Bulletin*, **67**, 2175-2193.

[11] Burke, K., Dessauvagie, T.F.J. and Whiteman, A.J. (1971) The Opening of the Gulf of Guinea and Geological History of the Benue Depression and Niger Delta. *Nature Physical Science*, **233**, 51-55. http://dx.doi.org/10.1038/physci233051a0

[12] Whiteman, A.J. (1982) Nigeria: Its Petroleum Geology, Resources and Potential. Graham and Trotman, London. http://dx.doi.org/10.1007/978-94-009-7361-9

[13] Billman, H.G. (1982) Offshore Stratigraphy and Paleontology of the Dahomey (Benin) Embayment, West Africa. *Nigerian Association of Petroleum Explorationists Bulletin*, **7**, 121-130.

[14] Coker, S.L., Ejedawe, J.E. and Oshiorienua, J.A. (1983) Hydrocarbon Source Potential of Cretaceous Rock of Okitipupa Uplift. *Nigerian Journal of Mining and Geology*, **2**, 163-169.

[15] Agagu, O.K. (1985) A Geological Guide to Bituminous Sediments in Southwestern Nigeria. Publication of Geology Department, University of Ibadan, Ibadan.

[16] Nton, M.E. (2001) Aspect of Rock Evaluation Studies of the Maastrichtian-Eocene Sediments. *Journal of Mining and Geology*, **13**, 33-39.

[17] Fayose, E.A. and Azeez, L.O. (1972) Micropalaeontological Investigations of Ewekoro Area, Southwestern Nigeria. *Micropaleontology*, **18**, 369-385. http://dx.doi.org/10.2307/1485014

[18] Brand, U. (1983) Mineralogy and Geochemistry of Deep Sea Clay in the Atlantic Ocean and Adjacent Seas and Ocean. *Geological Society of America Bulletin*, **76**, 803-832.

[19] Todd, T.W. (1966) Petrogenetic Classification of Carbonate Rocks. *Journal of Sedimentary Petrology*, **36**, 317-340.

[20] Marschner, H. (1968) Ca-Mg-Distribution in Carbonates from the Lower Keuper in NW-Germany. In: Muller, G. and Friedman, G.M., Eds., *Recent Developments in Carbonate Sedimentology in Central Europe*, Springer-Verlag, Berlin Heidelberg, 128-135. http://dx.doi.org/10.1007/978-3-642-88052-0_15